Environmental Research Letters

LETTER • **OPEN ACCESS**

Variability of particulate organic carbon in inland waters observed from MODIS Aqua imagery

To cite this article: Hongtao Duan *et al* 2014 *Environ. Res. Lett.* **9** 084011

View the article online for updates and enhancements.

Recent citations

- Using VIIRS/NPP and MODIS/Aqua data to provide a continuous record of suspended particulate matter in a highly turbid inland lake
Zhigang Cao *et al*

- Determination of the Downwelling Diffuse Attenuation Coefficient of Lake Water with the Sentinel-3A OLCI
Ming Shen *et al*

- Remote sensing estimation algorithm of diffuse attenuation coefficient applicable to different satellite data in Lake Taihu, China
SHEN Ming *et al*

This content was downloaded from IP address 5.171.17.94 on 18/03/2018 at 16:43

OPEN ACCESS
IOP Publishing
Environmental Research Letters
Environ. Res. Lett. 9 (2014) 084011 (10pp)
doi:10.1088/1748-9326/9/8/084011

Variability of particulate organic carbon in inland waters observed from MODIS Aqua imagery

Hongtao Duan[1], Lian Feng[2], Ronghua Ma[1], Yuchao Zhang[1] and Steven Arthur Loiselle[3]

[1] State Key Laboratory of Lake Science and Environment, Nanjing Institute of Geography and Limnology, Chinese Academy of Sciences, Nanjing 210008, People's Republic of China
[2] State Key Laboratory of Information Engineering in Surveying, Mapping and Remote Sensing, Wuhan University, Wuhan 430079, People's Republic of China
[3] Dipartimento Farmaco Chimico Tecnologico, CSGI, University of Siena, Siena, Italy

E-mail: htduan@niglas.ac.cn and htduan@gmail.com

Received 25 March 2014, revised 7 July 2014
Accepted for publication 21 July 2014
Published 19 August 2014

Abstract

Surface concentrations of particulate organic carbon (POC) in shallow inland lakes were estimated using MODIS Aqua data. A power regression model of the direct empirical relationship between POC and the atmospherically Rayleigh-corrected MODIS product ($R_{rc,645}$-$R_{rc,1240}$)/($R_{rc,859}$-$R_{rc,1240}$) was developed ($R^2 = 0.72$, RMSE = 35.86 μgL^{-1}, $p < 0.0001$, $N = 47$) and validated (RMSE = 44.46 μgL^{-1}, $N = 16$) with field data from 56 lakes in the Middle and Lower reaches of the Yangtze River, China. This algorithm was applied to an 11 year series of MODIS data to determine the spatial and temporal distribution of POC in a wide range of lakes with different trophic and optical properties. The results indicate that there is a general increase in minimum POC concentrations in lakes from middle to lower reaches of the Yangtze River. The temporal dynamics of springtime POC in smaller lakes were found to be influenced by local meteorological conditions, in particular precipitation and wind speed, while larger lakes were found to be more sensitive to air temperature.

Keywords: POC, algorithm, inland lakes, remote sensing, carbon cycling

1. Introduction

Lakes and inland water bodies are active, changing, and important regulators of the carbon cycle and global climate (Tranvik *et al* 2009). Collectively, nearly half as much organic carbon is buried in lakes globally as in the world's oceans, and small lakes (<500 km^2) account for 60–70% of this total organic carbon (TOC) burial (Alin and Johnson 2007). Particulate organic carbon (POC) is generally the form of carbon that most readily undergoes sedimentation and in-ecosystem loss. Even though POC is a small fraction of TOC present in most lakes (with respect to dissolved organic carbon, DOC), it plays an important role in sequestering carbon and associated compounds downward as part of the biological pump (Dhillon and Inamdar 2013, Son *et al* 2009). To better explore carbon cycling in the freshwater ecosystems and understand the fate of the main organic components, it is important to quantify POC as well as DOC effectively (Jiang *et al* 2012).

Satellite remote sensing observations provide a suitable means to explore temporal and spatial properties of inland lakes, allowing the possibility of measuring the limnological properties of many lakes simultaneously. Over the last three decades, significant contributions have been made to estimate the concentrations of phytoplankton pigments (e.g. chlorophyll a, Chla) using remote sensing (Clark 1981, Duan *et al* 2010, Mittenzwey *et al* 1992). However, the estimate of

Content from this work may be used under the terms of the Creative Commons Attribution 3.0 licence. Any further distribution of this work must maintain attribution to the author(s) and the title of the work, journal citation and DOI.

© 2014 IOP Publishing Ltd

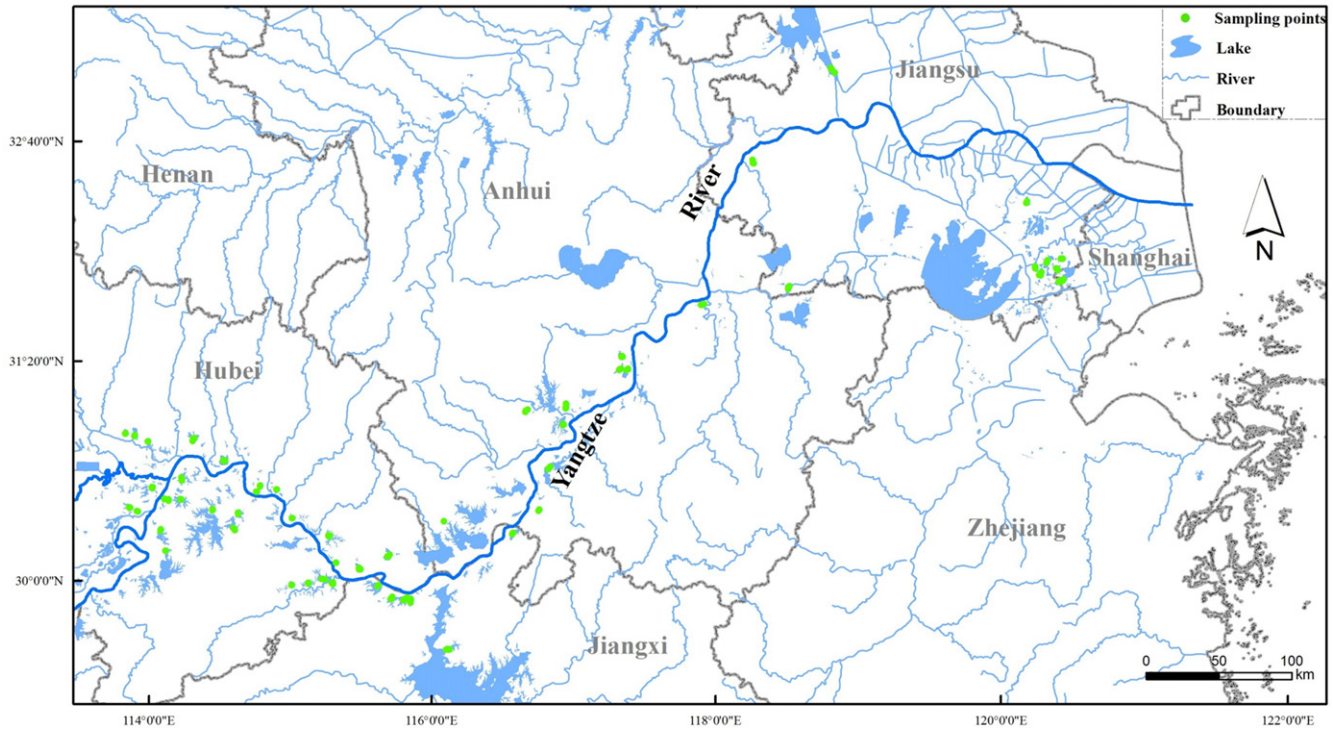

Figure 1. Locations of the 56 studied lakes along the Yangtze River, China.

total dissolved and particulate carbon presents a larger challenge, as optical properties of these two carbon pools can vary significantly in relation to their sources and sinks. The POC pool, in particular, may contain a wide variety of optically distinct components, from bacteria to macrophyte detritus (Morel and Ahn 1990) while the optical properties of DOC are highly sensitive to degradation processes (Loiselle *et al* 2009).

To better understand the C cycling in surface waters, algorithms have been developed to estimate POC concentrations in the open ocean (Gardner *et al* 2006, Mishonov *et al* 2003, Stramski *et al* 1999). In the first published algorithm for estimating POC from remote sensing, a two-step process was based on (Stramski *et al* 1999): (1) the dependence of the backscattering coefficient (b_{bp}) by particles suspended in seawater on the POC concentration; (2) the dependence of the spectral remote-sensing reflectance ($R_{rs}(\lambda)$) on b_{bp}. The resulting correlation was associated to the dominance of the biologically produced POC in controlling changes in b_{bp} in open oceans (Gardner *et al* 2006, Legendre and Michaud 1999). There are clear difficulties in applying this to turbid inland waters, where inorganic particles play a more important role in the optical backscattering properties of the water body (Ma *et al* 2009, Tzortziou *et al* 2007). Algorithms to estimate POC concentrations in inland waters remain a challenge.

The objective of the present study is to develop an optical algorithm for the retrieval of surface water POC concentrations in inland water bodies from satellite imagery. To our knowledge, this is the first estimate of POC concentrations in inland lakes using MODIS Aqua data.

2. Study region

The Yangtze River (known locally as Chang Jiang, or 'Long River'), is the longest river in Asia and third in the world (6300 km). The middle and lower reaches of the Yangtze River (28°50′–33°50′N and 113°30′–121°00′E, figure 1) have a total drainage area of about 8.0×10^4 km^2 (Chen *et al* 2001) which include some of the most important agricultural areas in China. The Middle and Lower Reaches of the Yangtze River basin (MLY) contain 529 lakes (areas $\geqslant$1 km^2), accounting for 18.57% of all lakes in China, with most water bodies (94.52%) less than 50 km^2 (Ma *et al* 2010, 2011).

In this study, field measurements were made in 56 lakes and used to develop a POC algorithm for inland water bodies (table 1 and figure 1). These lakes, distributed along the Yangtze River, are subject to various degrees of human impact from agricultural activities as well as effluent disposal from small villages and mega-urban areas, such as Wuhan and Nanjing.

3. Methods

3.1. Field data

Water samples and optical data were collected at 177 stations (3 or 4 stations per lake) by two survey groups using identical methodologies between 7 April and 20 April 2012. The selection of 56 sample lakes was made to be representative of water bodies along the MLY. Access to lakes for multiple sampling along a lake transect was also considered. POC

Table 1. Location, area, number of samples taken for each of the 56 lakes along the Yangtze River.

Lake	Long. (E)	Lat. (N)	Area	Num.	Lake	Long. (E)	Lat. (N)	Area	Num.
Taibai_HB	115.8100	29.9600	27.42	3	Zhupo	115.3842	29.8327	17.40	3
Wushan	115.5900	29.9000	15.81	3	Chi	115.7112	29.7875	59.43	3
Chidong	115.4010	30.1180	40.57	3	Changang	115.8817	29.6833	35.16	4
Makou	115.4292	29.9553	6.25	3	Shai	115.7925	29.7014	55.32	4
Che	115.1492	30.2541	9.06	3	Xinmiao	116.1621	29.3560	30.85	4
Wangtian	115.0587	30.4373	5.93	3	Qili	115.9297	29.6649	8.02	2
Baitan	114.9411	30.4691	5.13	3	Bali	115.9333	29.6864	9.33	4
HGdong	114.9135	30.4358	1.49	3	Taibo	116.7121	30.0110	24.76	3
Sanshan	114.7650	30.3160	23.97	3	Huangni	116.9269	30.1380	6.90	3
Baoan	114.7253	30.2229	45.46	3	Shenjin	117.0441	30.3920	96.09	3
Zhangdu	114.7084	30.643	36.24	3	Laincheng	117.2071	30.7398	8.70	4
Wu	114.4935	30.7963	27.50	3	Pogang	117.1765	30.6353	46.64	3
Wangmu	114.007	30.8662	7.93	3	Shanyasi	116.9160	30.7483	7.92	3
Yezhu	114.0718	30.8475	25.88	3	Fengsha	117.6243	30.92426	16.98	2
Baishui	114.1659	30.8036	13.39	3	Zhusi	117.6538	31.0026	11.52	3
WCdong	114.3827	30.561	34.35	3	Chenyao	117.6845	30.9199	20.01	3
Shangshe	114.218	30.132	10.24	3	Longwo	118.2874	31.2524	7.78	4
Lu	114.1971	30.2591	47.33	3	Kuncheng	120.7380	31.5794	17.51	3
Shanjiao	114.1679	30.5244	2.27	3	Yuandang	120.8820	31.0759	16.05	4
She	113.9871	30.4139	10.77	3	Dianshan	120.9172	31.0845	59.18	2
Guanlian	114.0416	30.3869	4.67	3	Bailian	120.9293	31.2083	5.08	3
Qingling	114.2447	30.447	7.21	3	Changbai	120.88681	31.1471	5.07	4
Huangjia	114.2736	30.4402	6.84	3	Cheng	120.81496	31.19764	43.59	3
Baoxie	114.5859	30.3534	25.32	3	Nanxing	120.74668	31.13363	4.96	4
Tangxun	114.3612	30.4341	44.83	3	Jiuli	120.7283	31.18104	2.91	4
Nantan	115.0972	29.8473	8.60	3	Gucheng	118.92217	31.27603	31.22	3
Zhulin	115.2192	29.8466	3.30	3	Shaobo	119.46619	32.57	103.73	4
Wang	115.3261	29.8637	42.87	3	Xuanwu	118.79939	32.06284	4.00	4

concentrations were determined by combustion of sample filters through pretreated 47 mm Whatman GF/F filters (6 h at 450 °C) by an EA3000 elemental analyzer. The filters were dried at 50 °C for 8 h and then wrapped in aluminum foil. Acidification treatment was performed to remove the carbonates from the filter, after which the filters were dried again and weighed. POC concentrations were measured by combustion of sample filters in an EA3000 elemental analyzer (Biddanda and Benner 1997).Chla concentrations were extracted using 90% ethanol and measured with a UV2401 spectrophotometer (Duan *et al* 2012, Gitelson *et al* 2008). Suspended particulate matter (SPM) concentrations were determined gravimetrically from samples collected on pre-combusted and pre-weighed GF/F filters with a diameter of 47 mm, dried at 95 °C overnight. SPM was differentiated into suspended particular inorganic matter (SPIM) and suspended particular organic matter (SPOM) by burning organic matter from the filters at 550 °C for 3 h and weighing the filters again (Duan *et al* 2012, 2014a).

3.2. Satellite data processing

Seven scenes of MODIS Aqua Level-0 (raw digital count) data were obtained from the US NASA Goddard Space Flight Center (GSFC) from 7 April 2012 to 20 April 2012 and therefore consistent with the field sampling. Level-0 data were processed using SeaDAS version 6.0 to generate calibrated at-sensor radiance. An initial attempt to use SeaDAS to generate above-water remote-sensing reflectance (R_{rs}) was unsuccessful. This was due to elevated aerosol concentrations and sun glint, even after adjusting processing options (e.g., the default limit of aerosol optical thickness at 869 nm was raised from 0.3 to 0.5, the default cloud albedo was raised from 2.7% to 4.0%, etc) (Feng *et al* 2012). Rayleigh-corrected reflectance $R_{rc,\lambda}$ was derived after correction for Rayleigh scattering and gaseous absorption effects as (Hu *et al* 2004):

$$R_{rc,\lambda} = \pi L_{t,\lambda}{}^{*} / \left(F_{0,\lambda} \times \cos\theta_0 \right) - R_{r,\lambda}, \quad (1)$$

where λ is the wavelength of the MODIS spectral band, L_t* is the calibrated at-sensor radiance after correction for gaseous absorption, F_0 is the extraterrestrial solar irradiance, θ_0 is the solar zenith angle, and R_r is the reflectance due to Rayleigh (molecular) scattering estimated using the 6S radiative transfer code. The R_{rc} data were geo-referenced into a cylindrical equidistance (rectangular) projection.

Concurrent datasets of MODIS reflectance data and *in situ* POC measurements were made using a time window of ±24 h between MODIS and *in situ* measurements. To avoid potential influence of patchiness in the optical properties of the measurement, a homogeneity test of the 3 × 3-pixel box centered at the *in situ* station was performed (note that each MODIS pixel represents 250 m × 250 m). If the variance of

Table 2. Water quality characteristics of the 56 lakes studied along the Yangtze River, China.

	Chla (μgL^{-1})	SPM (mgL^{-1})	SPOM (mgL^{-1})	SPIM (mgL^{-1})	POC (μgL^{-1})	DOC (mgL^{-1})
Min	0.55	1.39	0.68	0.59	16.63	0.94
Max	243.62	68.95	57.06	37.20	941.93	24.81
Mean	42.07	18.09	10.71	7.39	238.48	5.94
Stdev	45.72	11.95	9.68	5.76	146.84	3.66

the 3×3 box was >0.4, the corresponding matching pair was discarded from the regression. With this strict quality control criteria, a total of 63 matching pairs were selected. 47 samples (2/3) of this dataset were selected for training, while the other 16 samples were used for the algorithm validation.

The Normalized Difference Vegetation Index (NDVI), defined as $(R_{NIR}–R_{RED})/(R_{NIR}+R_{RED})$ was used to distinguish water bodies from surrounding dry soil or vegetation with threshold value set to zero (Haas *et al* 2009, Kaptué Tchuenté *et al* 2011). However, nonwater features in the NDVI image may not be completely eliminated in shallow turbid lakes. A modified NDVI threshold (<–0.05) was used to provide more accurate estimates of lake borders (Ma *et al* 2011).

3.3. Statistical analysis

Daily data of precipitation rate (mm), wind speed (ms^{-1}) and air temperature (°C) were obtained from the China Meteorological Data Sharing Service System (http://cdc.cma.gov.cn/). Distance between lakes was determined using the 'haversine' formula (Rick 1999). Correlations between POC estimates, distance and meteorological data were identified using a linear model where direct correlations (increasing) had positive Pearson correlation coefficients (r) and indirect correlations (decreasing) had negative coefficients. A multiple regression of POC estimates with meteorological data was performed using a linear least squares fitting procedure.

4. Results and discussion

4.1. POC sources in inland waters

Field data indicated a large variability in the properties of 56 lakes studied, with a 50-fold range in POC (17–942 μgL^{-1}), a 60-fold range in SPM (1.39–68.95 mgL^{-1}), a 400 fold range in Chla (0.55–240 μgL^{-1}) (table 2, figure 2). The average Chla concentration was high, 42 μgL^{-1}, as would be expected from an area which includes hyper-eutrophic waterbodies such as Lakes Taihu and Chaohu (Duan *et al* 2009, Jin *et al* 2012). SPM concentrations were dominated by SPOM, indicating that plankton and resuspended organic matter played an important role (Upsdell, 2005). POC correlated well with SPM ($r = 0.88$) and SPOM ($r = 0.80$) (figure 3(a)). Generally, the organic content of suspended matter from terrigenous sources can be expected to have a similar organic carbon content (Cauwet and Mackenzie, 1993). The correlation between POC and Chla ($r = 0.27$, figure 3(b)) was low, indicating that phytoplankton was not the dominant source particulate carbon in these waters. The mean ratio of DOC to POC concentrations indicated that DOC accounted for 96% of TOC in the study lakes.

The ratio of POC to SPM (POC%) was used to describe the relative fraction of organic matter composing the suspended particulate matter assemblage. The POC:Chla ratio was used to describe the relative proportion of organic material (both living and nonliving) relative to autotrophic organisms. The latter index is also influenced by variations in the intracellular photosynthetic pigment concentrations when diverse water bodies are compared (Loisel and Morel 1998, Vantrepotte *et al* 2012). POC% ranged between 0.80% and 2.66% (average at 1.44%) (figure 2(d)), which is similar to that reported for the Yellow River (0.50%–5.00%) (Zhang *et al* 2012). The POC:Chla ratio of the 56 lakes averaged 13 (0.75–157) (figure 2(e)), much smaller than that measured in Yangtze River (48–136) or similar rivers globally (Yellow River: 3988; lower Mississippi River: 256) (Duan and Bianchi, 2006, Zhang *et al* 2012), typical coastal waters (Charente estuary: 232–13 152; English Channel, Southern North Sea and French Guiana: 24–686) (Modéran *et al* 2012, Vantrepotte *et al* 2012), or marine waters (20–200) (Cifuentes *et al* 1988).

Freshwater ecosystems receive organic matter from two distinct sources: primary production occurring within the waterbody (autochthonous production) and external loading of terrestrial organic matter from the watershed (allochthonous loading) (Prokushkin *et al* 2011). As the POC concentrations were well correlated to the concentrations of SPM and SPOM but poorly correlated to Chla, the source of POC in many of these lakes was more closely tied to catchment sources or resuspended organic detritus. These lakes were small- to moderate-sized and surrounded by highly productive wetlands and agricultural lands that represent major sources of organic matter loading (Wetzel 1984). It should be noted that allochthonous and autochthonous POC sources will vary seasonally, typically with maximum phytoplankton production in summer and peak allochthonous inputs in the fall (Bianchi and Argyrou 1997, Cauwet and Mackenzie 1993).

4.2. POC algorithm development

Several POC algorithms have been proposed in the past, including the semi-analytical algorithms based on radiative transfer theory and empirical regression algorithms (Gardner *et al* 2006, Son *et al* 2009, Stramski *et al* 1999). However, these algorithms were developed for ocean waters and rely on the dominance of phytoplankton biomass in the total POC concentration (Morel 1988, Pabi and Arrigo 2006). The optical properties of these study lakes were influenced not

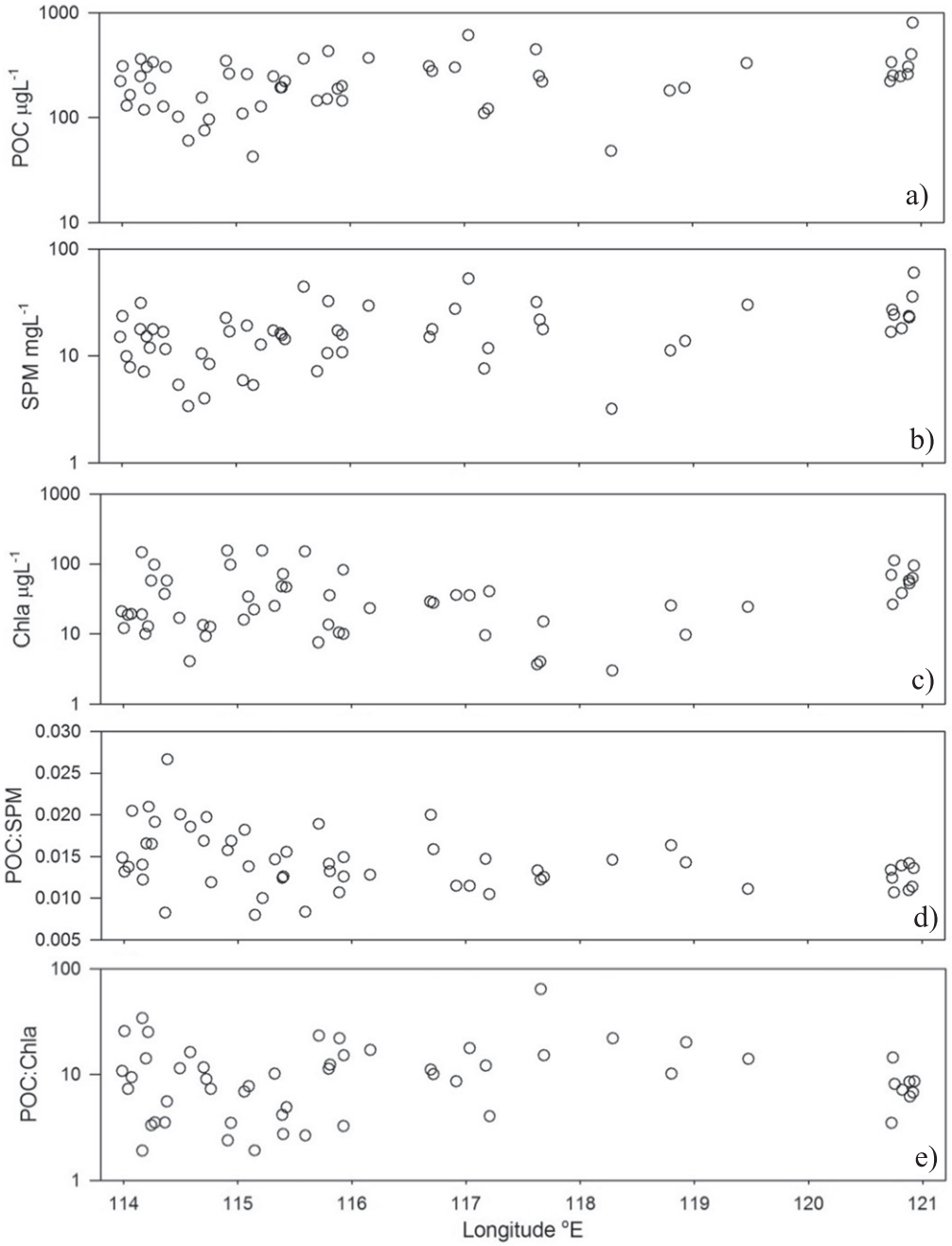

Figure 2. Characteristics of suspended particulate matter measured on surface samples in 56 lakes along the Yangtze River, China. From top to the bottom, the graphs show the concentration of particulate organic carbon (POC), the concentration of suspended particulate matter (SPM), the concentration of chlorophyll-a (Chla), the ratio of POC to SPM, and the ratio of POC to Chla. Average values for each lake are shown.

only by phytoplankton and related (co-varying) particles, but also by inorganic particles and organic detritus (Duan *et al* 2014a, IOCCG 2000). Hence, new algorithms were required for these more complex optical conditions and multiple POC sources.

As typical ocean bands often saturate over turbid lake waters, an approach using MODIS land bands to determine $R_{rc,\lambda}$ was developed. Regressions between *in* situ POC and single-band $R_{rc,\lambda}$ showed a very poor correlation ($r<0.4$), suggesting that aerosol contributions could not be ignored. In addition to the single-band algorithms, simple band-ratios were also explored but did not provide strong correlations.

Aerosol contributions to the satellite signal vary spatially along the Yangtze River (He *et al* 2010). Water reflectance at 1240 nm is virtually null in coastal and inland waters (Hu *et al* 2000). Assuming spectrally consistent but spatially variable impacts of aerosols, reflectance bands were corrected for aerosols using $R_{rc,1240}$ (Feng *et al* 2012). For the atmospherically corrected data, $(R_{rc,645}–R_{rc,1240})/(R_{rc,859}–R_{rc,1240})$ showed the best relationship with POC concentrations

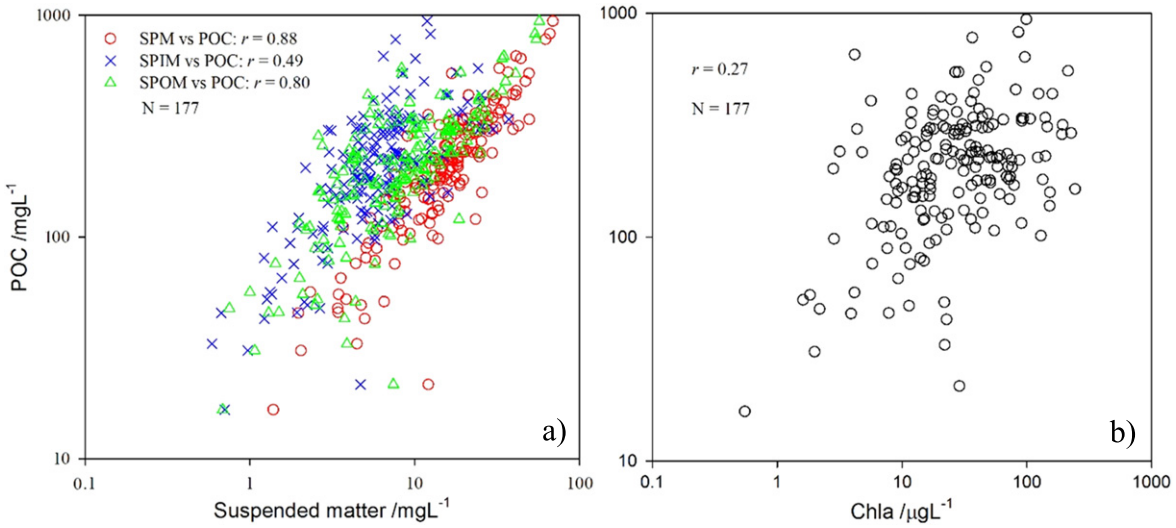

Figure 3. Relationship between the concentrations of POC and: (a) suspended matter ([POC] = 10.88[SPM] + 42.29, $N = 177$, $R^2 = 0.78$, $p < 0.001$); (b) Chlorophyll-a.

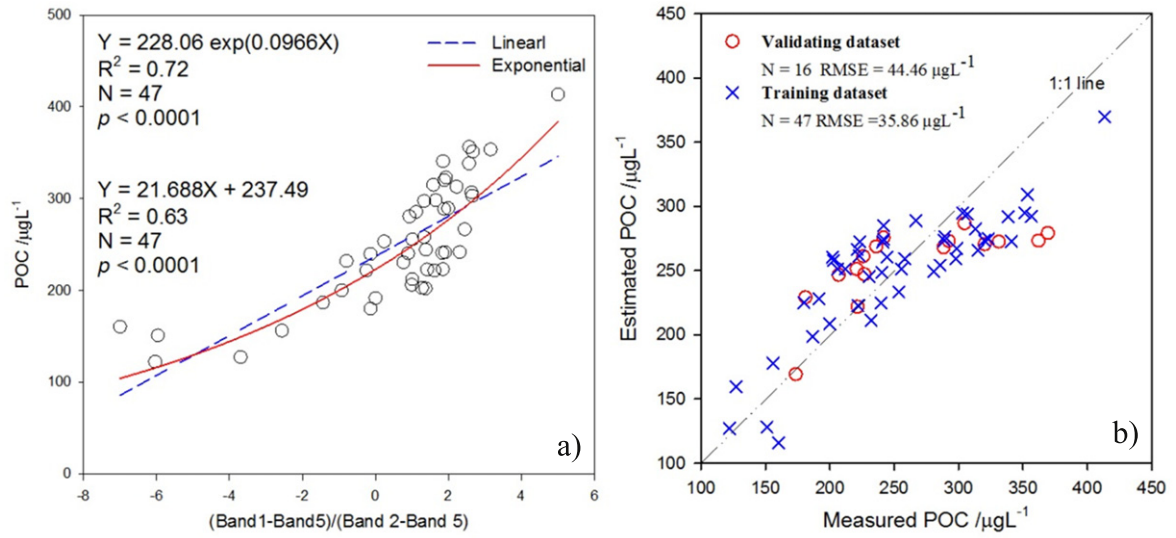

Figure 4. Relationships between surface concentration of particulate organic carbon, POC, and MODIS reflectance ratios: (a) algorithm developed; (b) validation result. Note that Rayleigh-corrected reflectance $R_{rc,\lambda}$ was used herein and their combination $(R_{rc,645}\text{-}R_{rc,1240})/(R_{rc,859}\text{-}R_{rc,1240})$ showed the best relationship with POC concentrations.

($R^2 = 0.72$, $p < 0.0001$) (figure 4(a), equation (2)). The fitted POC algorithm was:

$$\mathrm{POC}\left(\mu g\ \mathrm{L}^{-1}\right) = 228.06 \exp\left[0.0966 \times \left(R_{rc,645} - R_{rc,1240}\right)\Big/\left(R_{rc,859} - R_{rc,1240}\right)\right] \quad (2)$$

The validation of this relationship showed a strong correlation between *in situ* measured POC and MODIS estimated POC (figure 4(b)).

This is the first algorithm focused on POC dominated by detrital matter. It should be noted that this algorithm was developed and tested for the POC present in predominantly shallow lakes in the period of the year when algal blooms are low (Duan *et al* 2014b, 2009). To best capture the seasonal variability of POC in these lakes, additional efforts would be required to develop and test POC algorithms for periods of algal blooms (May–August) and periods of low winds (October–November). Correction using $R_{rc,1240}$ would be important in both cases to reduce the effect of seasonal variation in atmospheric conditions. The resulting seasonal set of POC algorithms could be adapted for routine processing of MODIS data to produce maps of surface POC in these lakes using the same empirical approach.

Optical wavebands in the red and NIR have been widely used to examine different types of particulates, including floating algal biomass (Hu *et al* 2010), general turbidity (Chen *et al* 2007), dredging water plumes (Kutser *et al* 2007), SPM (Feng *et al* 2012) and Chla concentrations (Dall'Olmo *et al* 2005). To date, these approaches have been most success when there is one dominating particulate, as they do not allow for differentiation between high concentrations of POC, Chla or SPM.

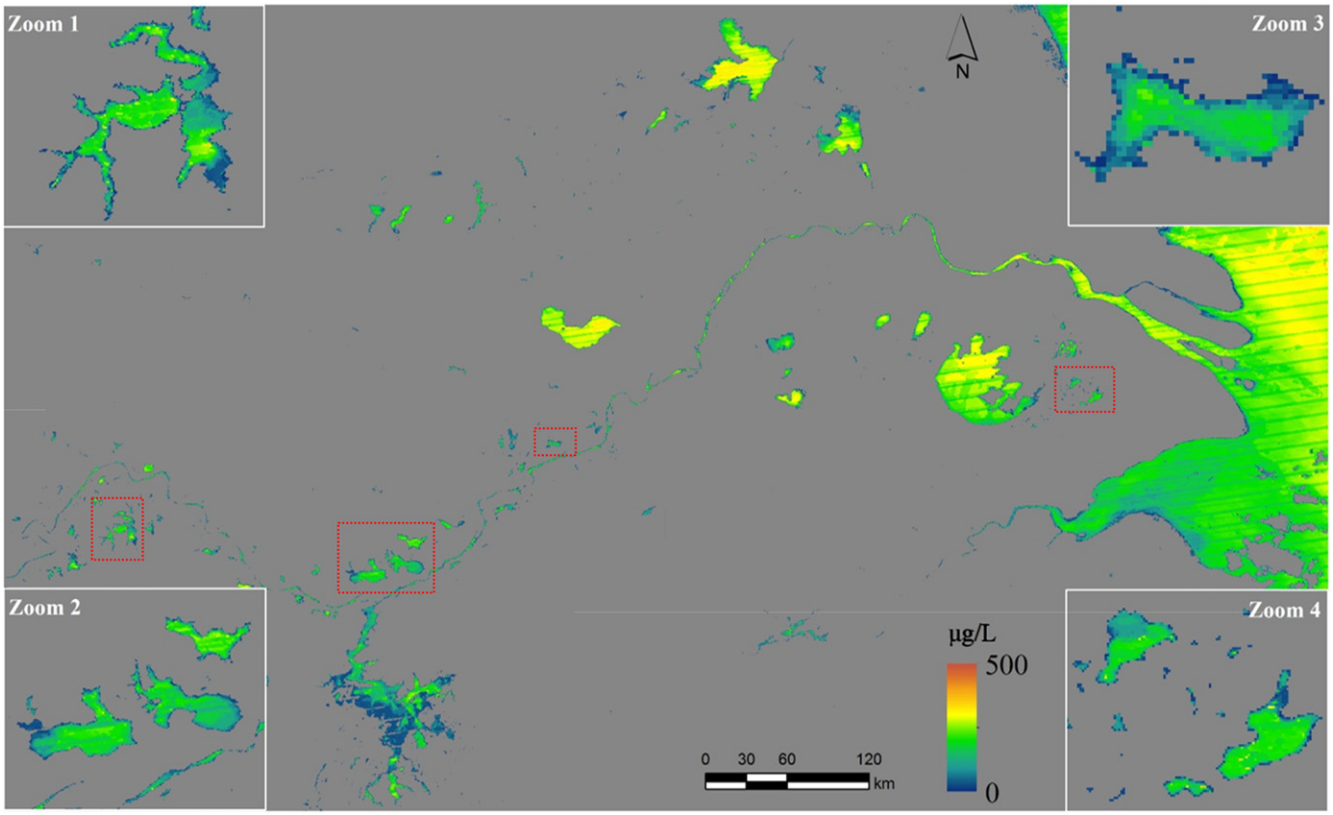

Figure 5. Mean MODIS-derived POC distributions in April between 2003 and 2013. Zoom 1: Lake Liangzi; Zoom 2: Lake Longgan, Lake Huangda and Lake Bo; Zoom 3: Lake Baidang; Zoom 4: Lake Chen and Lake Dianshan.

MODIS images have been used widely in routine monitoring of oceanic, coastal and inland lakes (Feng *et al* 2014, Hu *et al* 2012, Zhang *et al* 2010). To monitor lakes across a range of sizes requires the spatial resolution of the 250 and 500 m bands. However, the spectral resolution of the 250 and 500 m bands limits their use of lake color assessment, compared to the more appropriate spectral characteristics of the 1000 m bands (Kaptué *et al* 2013, Olmanson *et al* 2011). Nonetheless, our analysis shows that it is possible to develop appropriate algorithms to monitor key carbon components of complex inland waters using the spectral characteristics of the MODIS 250 and 500 m bands, taking advantage of its high temporal resolution and wide swath.

4.3. Inter-annual variability of POC

The POC algorithm (equation (2)) and water area-delineation methods developed for the April 2012 dataset were then used with Rayleigh-corrected reflectance to explore a series of MODIS Aqua images from 2003 to 2013 (figure 5). All images were obtained in the same month (April) of each year to minimize seasonal variations in aquatic optical conditions (e.g. algal blooms) (Duan *et al* 2014b, 2009). The number of lakes explored in each image depended on the presence of clouds. The average POC concentrations for each lake were used to examine the inter-annual variability of all lakes in the MLY. Only lakes with at least 5 measurements in the 11-year dataset were considered. These lakes (55) were located throughout the MLY and represented a wide range of lake conditions, with lake area ranging from 0.32 to 2508 km^2. The yearly lake POC averages demonstrated a high inter-annual variability, with POC concentrations generally highest in 2013 and lowest in 2004 (figure 6(a)). Interannual variability of individual lakes was compared to local meteorological data (rain, wind, and air temperature) to identify commonalities.

Lakes were grouped according to lake size in four categories: less than 5 km^2, between 5 km^2 and 25 km^2, between 25 km^2 and 100 km^2, and above 100 km^2 (figure 6(a)). The inter-annual POC dynamics of each lake category were compared to average meteorological conditions. Direct correlations were identified for one lake size category ($n = 11$, $p < 0.01$). The inter-annual POC concentrations in the third lake category (25 km^2 < lake area < 100 km^2) were found to be well described by a linear equation that included the maximum air temperature on the preceding day of measurement (day2-maxtemp, 0.1 °C) (POC = 322 − 0.40 day2-maxtemp, $R^2 = 58\%$, F-ratio = 4.49, $p = 0.006$), indicating the higher sensitivity of these water bodies to temperature and mixing. Comparisons using multiple linear regression indicated that the inter-annual POC concentrations in the smaller lake category (lake area < 5 km^2) were found to be well described by linear combination of precipitation on the day of estimation (day-rain, 0.1 mm), on the preceding day (day2-rain) and wind speed on the same day (wind, 0.1 ms^{-1}) (POC = 274 − 0.99 wind + 0.40 day2-rain − 20.0 day-rain, $R^2 = 86\%$, F-

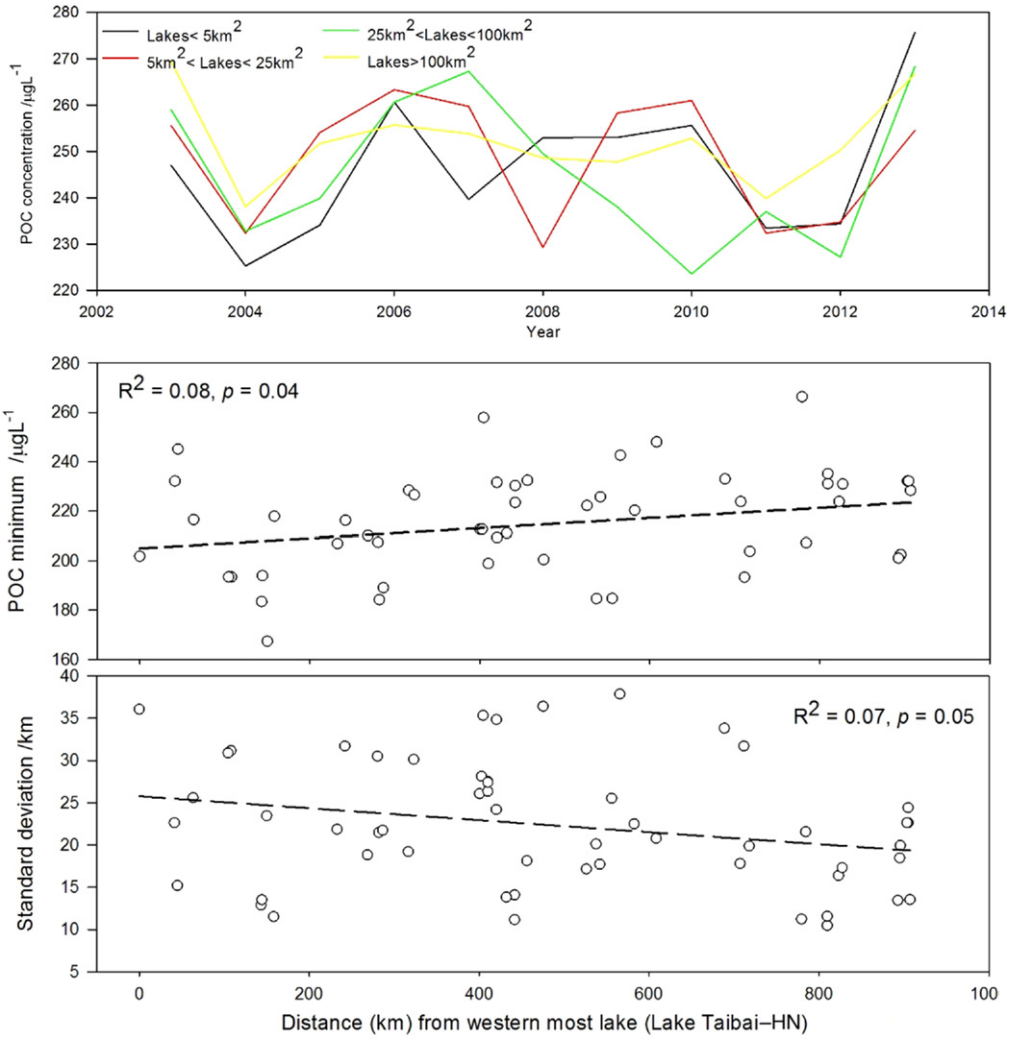

Figure 6. (a) Inter-annual dynamics of average POC concentrations of different lake size categories. (b) Relationship between geographic position in MLY and POC concentrations (lake averages) estimated using MODIS data.

ratio = 14.65, $p = 0.002$) indicating the sensitivity of these water bodies to mixing, run-off and dilution.

Spatially, there was a low correlation between lake geographic position in the MLY and its POC concentration (figure 6(b)). While the specific catchment land cover for each lake was not determined, the general trend from the Middle to Lower Yangtze is one of increasing crops cover and decreasing pasture cover (Ellis *et al* 2010). The minimum POC concentrations in the 11-year dataset of each of the 56 lakes were positively correlated ($n = 56$, $r = 0.28$, $p = 0.03$) to increasing distance from Lake Taibai_HN, the westernmost study lake in the Middle Yangtze (29.0 °N, 112.1 °E) (figure 1). In addition, the standard deviations of 11-year POC dataset for each lake were negatively correlated ($n = 56$, $r = -0.26$, $p = 0.05$) with distance from Lake Taibai_HN. These correlations indicated a general tendency for diminished inter-annual variability of POC and higher minimum POC in lakes of the Lower Yangtze. Higher agricultural activity favors increased nutrient inputs (promoting autochthonous POC production) as well as increased sediment inputs (including allochthonous POC) (Martinuzzi *et al* 2014). A more detailed study of individual catchments of each lake would provide a more complete analysis of the causes of inter-lake differences.

5. Conclusions

An empirical approach used to examine the surface concentrations of POC in inland lakes using optical remote sensing data was demonstrated to be robust. Among the algorithms examined, a power relation of the atmospherically Rayleigh-corrected reflectances at 645 nm, 859 nm and 1240 nm was found to provide the most accurate estimates. The algorithm provided good estimates of POC concentrations across a range of inland lakes over a large geographical area. This algorithm was used to study the inter-annual and spatial variation of POC concentrations of a large number of lakes, with varying characteristics, and provided new information on the dynamics of this important component of the aquatic carbon cycle. The data series was limited to a single

month (April) that is characterized by higher winds, lower rain and low algal blooms in the MLY lakes.

Acknowledgements

The authors would like to thank all participants and voluntary contributors (Feizhou Chen, Min Zhang, Guangjia Jiang, Jiahui Huang and Changfeng Wang (Nanjing Institute of Geography and Limnology, Chinese Academy of Sciences: NIGLAS)). Thank also for climate data provided by the China Meteorological Data Sharing Service System (http://cdc.cma.gov.cn/), and MODIS data provided by the NASA ocean color web (http://oceancolor.gsfc.nasa.gov/). This study was support by the National High Technology Research and Development Program of China (2014AA06A509), the National Natural Science Foundation of China (41171271, 41171273 and 41101316), the ESA-MOST Dragon 3 Cooperation program (10561) and the 135-Program (NIGLAS2012135014 and NIGLAS2012135010).

References

Alin S and Johnson T C 2007 Carbon cycling in large lakes of the world: a synthesis of production, burial, and lake-atmosphere exchange estimates *Glob. Biogeochem. Cycl.* **21** GB3002

Bianchi T and Argyrou M 1997 Temporal and spatial dynamics of particulate organic carbon in the Lake pontchartrain estuary, southeast louisiana, USA *Estuarine, Coastal Shelf Sci.* **45** 557–69

Biddanda B and Benner R 1997 Carbon, nitrogen, and carbohydrate fluxes during the production of particulate and dissolved organic matter by marine phytoplankton *Limnol. Oceanogr.* **42** 506–18

Cauwet G and Mackenzie F 1993 Carbon inputs and distribution in estuaries of turbid rivers: the Yang Tze and Yellow rivers (China) *Mar. Chem.* **43** 235–46

Chen Z, Li J, Shen H and Zhanghua W 2001 Yangtze River of China: historical analysis of discharge variability and sediment flux *Geomorphology* **41** 77–91

Chen Z Q, Hu C M and Muller-Karger F 2007 Monitoring turbidity in tampa bay using MODIS/Aqua 250 m imagery *Remote Sens. Environ.* **109** 207–20

Cifuentes L A, Sharp J H and Fogel M L 1988 Stable carbon and nitrogen isotope biogeochemistry in the delaware estuary *Limnol. Oceanogr.* **33** 1102–15

Clark D K 1981 Phytoplankton pigment algorithms for the Nimbus-7 CZCS(coastal zone color scanner) *Oceanography From Space: Marine Science* (New York: Springer) pp 227–37

Dall'Olmo G, Gitelson A A, Rundquist dc, Leavitt B, Barrow T and Holz J C 2005 Assessing the potential of SeaWiFS and MODIS for estimating chlorophyll concentration in turbid productive waters using red and near-infrared bands *Remote Sens. Environ.* **96** 176–87

Dhillon G S and Inamdar S 2013 Extreme storms and changes in particulate and dissolved organic carbon in runoff: Entering uncharted waters? *Geophys. Res. Lett.* **40** 1322–7

Duan H, Ma R and Hu C 2012 Evaluation of remote sensing algorithms for cyanobacterial pigment retrievals during spring bloom formation in several lakes of East China *Remote Sens. Environ.* **126** 126–35

Duan H, Ma R, Loiselle S A, Shen Q, Yin H and Zhang Y 2014a Optical characterization of black water blooms in eutrophic waters *Sci. Total Environ.* **482–483** 174–83

Duan H, Ma R, Zhang Y and Loiselle S A 2014b Are algal blooms occurring later in Lake Taihu? Climate local effects outcompete mitigation prevention *J. Plankton Res.* **36** 866–71

Duan H T *et al* 2009 Two-decade reconstruction of algal blooms in China's Lake Taihu *Environ. Sci. Technol.* **43** 3522–8

Duan H T *et al* 2010 A new three-band algorithm for estimating chlorophyll concentrations in turbid inland lakes *Environ. Res. Lett.* **5** 044009

Duan S and Bianchi T S 2006 Seasonal changes in the abundance and composition of plant pigments in particulate organic carbon in the lower Mississippi and Pearl Rivers *Estuaries Coasts* **29** 427–42

Ellis E C, Goldewijk K K, Siebert S, Lightman D and Ramankutty N 2010 Anthropogenic transformation of the biomes, 1700 to 2000 *Glob. Ecol. Biogeogr.* **19** 589–606

Feng L, Hu C, Chen X and Song Q 2014 Influence of the three gorges dam on total suspended matters in the Yangtze Estuary and its adjacent coastal waters: observations from MODIS *Remote Sens. Environ.* **140** 779–88

Feng L, Hu C, Chen X, Tian L and Chen L 2012 Human induced turbidity changes in poyang lake between 2000 and 2010: observations from MODIS *J. Geophys. Res.* **117** C07006

Gardner W D, Mishonov A and Richardson M J 2006 Global POC concentrations from in-situ and satellite data *Deep-Sea Research Part Ii-Topical Studies in Oceanography* **53** 718–40

Gitelson A A *et al* 2008 A simple semi-analytical model for remote estimation of chlorophyll-a in turbid waters: Validation *Remote Sens. Environ.* **112** 3582–93

Haas E M, Bartholome E and Combal B 2009 Time series analysis of optical remote sensing data for the mapping of temporary surface water bodies in sub-Saharan western Africa *J. Hydrol.* **370** 52–63

He Q S, Li C C, Tang X, Li H L, Geng F H and Wu Y L 2010 Validation of MODIS derived aerosol optical depth over the Yangtze River Delta in China *Remote Sens. Environ.* **114** 1649–61

Hu C, Cannizzaro J, Carder K L, Muller-Karger F E and Hardy R 2010 Remote detection of Trichodesmium blooms in optically complex coastal waters: examples with MODIS full-spectral data *Remote Sens. Environ.* **114** 2048–58

Hu C, Carder K L and Muller-Karger F E 2000 Atmospheric correction of seaWiFS imagery over turbid coastal waters: a practical method *Remote Sens. Environ.* **74** 195–206

Hu C, Chen Z, Clayton T D, Swarzenski P, Brock J C and Muller-Karger F E 2004 Assessment of estuarine water-quality indicators using MODIS medium-resolution bands: initial results from tampa bay, FL *Remote Sens. Environ.* **93** 423–41

Hu C, Lee Z and Franz B 2012 Chlorophyll a algorithms for oligotrophic oceans: A novel approach based on three-band reflectance difference *J. Geophys. Res.: Oceans* **117** C01011

IOCCG 2000 Remote sensing of ocean colour in coastal, and other optically-complex, waters ed S Sathyendranath *Reports of the International Ocean Colour Coordinating Group* No. 3 (Dartmouth, Canada: IOCCG)

Jiang G, Ma R, Loiselle S A and Duan H 2012 Optical approaches to examining the dynamics of dissolved organic carbon in optically complex inland waters *Environ. Res. Lett.* **7** 034014

Jin J W, Duan H T, Zhao C L, Zhou L, Shang L L and Jiang G J 2012 Remote estimation of phytoplankton pigments in inland lake waters with algae *J. Infrared Millim. Waves* **31** 132–6

Kaptué A T, Hanan N P and Prihodko L 2013 Characterization of the spatial and temporal variability of surface water in the Soudan-Sahel region of Africa *J. Geophys. Res.: Biogeosci.* **118** 1–12

Kaptué Tchuenté A T, De Jong S M, Roujean J-L, Favier C and Mering C 2011 Ecosystem mapping at the African continent

scale using a hybrid clustering approach based on 1 km resolution multi-annual data from SPOT/VEGETATION *Remote Sens. Environ.* **115** 452–64
Kutser T, Metsamaa L, Vahtmäe E and Aps R 2007 Operative monitoring of the extent of dredging plumes in coastal ecosystems using MODIS satellite imagery *J. Coast. Res.* **SI 50** 180–4
Legendre L and Michaud J 1999 Chlorophyll a to estimate the particulate organic carbon available as food to large zooplankton in the euphotic zone of oceans *J. Plankton Res.* **21** 2067–83
Loisel H and Morel A 1998 Light scattering and chlorophyll concentration in case 1 waters: a reexamination *Limnol. Oceanogr.* **43** 847–58
Loiselle S A, Bracchini L, Cozar A, Dattilo A M, Tognazzi A and Rossi C 2009 Variability in photobleaching yields and their related impacts on optical conditions in subtropical lakes *J. Photochem. Photobiol. B-Biol.* **95** 129–37
Ma R H *et al* 2010 A half-century of changes in China's lakes: Global warming or human influence? *Geophys. Res. Lett.* **37** L24106
Ma R H *et al* 2011 China's lakes at present: Number, area and spatial distribution *Sci. China-Earth Sci.* **54** 283–9
Ma R H, Pan D L, Duan H T and Song Q J 2009 Absorption and scattering properties of water body in Taihu Lake, China: backscattering *Int. J. Remote Sens.* **30** 2321–35
Martinuzzi S *et al* 2014 Threats and opportunities for freshwater conservation under future land use change scenarios in the United States *Glob. Change Biol.* **20** 113–24
Mishonov A V, Gardner W D and Richardson M J 2003 Remote sensing and surface POC concentration in the South Atlantic *Deep-Sea Research Part Ii-Topical Studies in Oceanography* **50** 2997–3015
Mittenzwey K H, Gitelson A A and Kondratiev K Y 1992 Determination of chlorophyll-a of inland waters on the basis of spectral reflectance *Limnol. Oceanogr.* **37** 147–9
Modéran J, David V, Bouvais P, Richard P and Fichet D 2012 Organic matter exploitation in a highly turbid environment: planktonic food web in the charente estuary, france *Estuarine, Coastal Shelf Sci.* **98** 126–37
Morel A 1988 Optical modeling of the upper ocean in relation to its biogenous matter content (case-I waters) *J. Geophys. Res.: Oceans* **93** 10749–68
Morel A and Ahn Y-H 1990 Optical efficiency factors of free-living marine bacteria: Influence of bacterioplankton upon the optical properties and particulate organic carbon in oceanic waters *J. Mar. Res.* **48** 145–75
Olmanson L G, Brezonik P L and Bauer M E 2011 Evaluation of medium to low resolution satellite imagery for regional lake water quality assessments *Water Resour. Res.* **47** W09515
Pabi S and Arrigo K R 2006 Satellite estimation of marine particulate organic carbon in waters dominated by different phytoplankton taxa *J. Geophys. Res.: Oceans* **111** C09003
Prokushkin A S *et al* 2011 Sources and the flux pattern of dissolved carbon in rivers of the Yenisey basin draining the Central Siberian Plateau *Environ. Res. Lett.* **6** 045212
Rick D 1999 Deriving the haversine formula *The Math Forum* www.movable-type.co.uk/scripts/latlong.html
Son Y B, Gardner W D, Mishonov A V and Richardson M J 2009 Multispectral remote-sensing algorithms for particulate organic carbon (POC): The gulf of Mexico *Remote Sens. Environ.* **113** 50–61
Stramski D, Reynolds R A, Kahru M and Mitchell B G 1999 Estimation of particulate organic carbon in the ocean from satellite remote sensing *Science* **285** 239–42
Tranvik L J *et al* 2009 Lakes and reservoirs as regulators of carbon cycling and climate *Limnol. Oceanogr.* **54** 2298–314
Tzortziou M, Subramaniam A, Herman J R, Gallegos C L, Neale P J and Harding L W 2007 Remote sensing reflectance and inherent optical properties in the mid Chesapeake Bay *Estuarine Coastal Shelf Sci.* **72** 16–32
Upsdell B 2005 The carbon and nitrogen composition of suspended particulate matter in lake erie, selected tributaries, and its outflow (Ontario, Canada: University of Waterloo)
Vantrepotte V, Loisel H, Dessailly D and Mériaux X 2012 Optical classification of contrasted coastal waters *Remote Sens. Environ.* **123** 306–23
Wetzel R G 1984 Detrital dissolved and particulate organic-carbon functions in aquatic ecosystems *Bull. Mar. Sci.* **35** 503–9
Zhang L J, Wang L, Cai W J, Liu D M and Yu Z G 2012 Organic carbon transport and impacts of human activities in the Yellow River *Biogeosci. Discuss.* **9** 14365–405
Zhang M W, Tang J W, Dong Q, Song Q T and Ding J 2010 Retrieval of total suspended matter concentration in the Yellow and East China Seas from MODIS imagery *Remote Sens. Environ.* **114** 392–403